Supplementary Information (SI) for CrystEngComm.
This journal is © The Royal Society of Chemistry 2024

ELECTRONIC SUPPLEMENTARY INFORMATION

Hexadecanuclear isobutyrate nanoclusters with a $\{Co^{II}_{14}Co^{III}_{2}\}$ core

Dumitru Stati,[a] Jan van Leusen,[b] Victor Ch. Kravtsov,[a] Karl Krämer,[c] Shi-Xia Liu,[c] Silvio Decurtins,[c] Paul Kögerler[b] and Svetlana G. Baca[a]*

[a]Institute of Applied Physics, Moldova State University, Academiei str. 5, MD2028 Chisinau, R. Moldova

[b]Institute of Inorganic Chemistry, RWTH Aachen University, Landoltweg 1, 52074 Aachen, Germany

[c]Department of Chemistry, Biochemistry and Pharmaceutical Sciences, W. Inäbnit Laboratory for molecular quantum materials, University of Bern, CH-3012 Bern, Switzerland

Corresponding Author:

* S.G.B. E-mail: svetlana.baca@ifa.usm.md; sbaca_md@yahoo.com

Table S1. Coordination compounds with a {Co_{16}} core……..…….3-4
Table S2. Crystallographic data and structure refinement parameters for **1**–**2**……..……..…5
Table S3. Selected bond distances (in Å) for **1**–**2**…….6-7
Table S4. Hydrogen bonds geometry (Å, deg) for **1**–**2**…….……7
Table S5. BVS calculations for Co atoms in **1**–**2**……....8
Table S6. Hirshfeld surfaces for the Co(II) and Co(III) centers in **1**……....9
Table S7. Hirshfeld surfaces for the Co(II) and Co(III) centers in **2**……...10
Table S8. Quantitative data from Hirshfeld surface of the of the Co(II) and Co(III) centers in **1**-**2**……11
Figure S1. IR spectrum of **1**.……...12
Figure S2. IR spectrum of **2**……12
Figure S3. TGA/DSC curves for **1**……..13
Figure S4. TGA/DTG curves for **2**……..…13
Figure S5. PRDX analysis of **1**……14
Figure S6. PRDX analysis of **2**……14
Figure S7. Experimental and simulated (insert) isotope patterns for **1**…….…….…….15
Figure S8. Asymmetric unit of nanocluster **1**…….…….…….16
Figure S9. Asymmetric unit of nanocluster **2**…….…….....16
Figure S10. View of the Hirshfeld surface for nanocluster in **1**…..…..…….…….…….17
Figure S11. View of the Hirshfeld surface nanocluster in **2**…….…….…….…..…18
Figure S12. 2D fingerprint plots and d_{norm} surface plots of the {Co_{16}} cluster in **2**……19
Figure S13. Hirshfeld surfaces for the Co(III) and Co(II) centres presenting different shapes in **1**……20
Figure S14. Hirshfeld surfaces for the Co(III) and Co(II) centres presenting different shapes in **2**……...…….…….……..…….……21

Table S1. Coordination compounds with a $\{Co_{16}\}$ core

	Cod	Core	Topology	Properties	References
1	AQOLOK AQOLOK01	$\{Co^{II}_8Co^{III}_8\}$	Metallocages	Photocatalyst	Y. Jin, H. Jiang, X. Tang, W. Zhang, Y. Liu, Y. Cui. *Dalton Trans*. **2021**, *50*,8533. https://doi.org/10.1039/D1DT00652E
2	CIHFOQ	$\{Co^{II}_{16}\}$	Face-centered cube with two wings	Antiferromagnetic $Co^{II}\cdots Co^{II}$ exchange interactions	Y. Cao, Y. Chen, L. Li, D. Gao, W. Liu, H. Hu, W. Li, Y. Li, *Dalton Trans*., **2013**, *42*, 10912, https://doi.org/10.1039/C3DT51140E
3	EGAHEC	$\{Co^{II}_{16}\}$	Metallocages	High-performance proton-conductive materials	T.-T. Guo, D.-M. Cheng, J. Yang, X. Xu, J.-F. Ma, *Chem. Commun.*, **2019**, *55*, 6277, https://doi.org/10.1039/C9CC01828J
4	EGAHIG				
5	EKIJAK	$\{Co^{II}_{16}\}$	Wheel-like phosphonate cluster	Magnetic properties: frequency-dependent out-of-phase signals below 3 K	Y.-Sh. Ma, Y. Song, X.-Y. Tang, R.-X. Yuan, *Dalton Trans*., **2010**, *39*, 6262, https://doi.org/10.1039/B923494B
6	EQOBAQ	$\{Co^{II}_{16}\}$	Metallocages	Highly soluble cages	M. R. Dworzak, M. M. Deegan, G. P. A. Yap, E. D. Bloch, *Inorg. Chem.*, **2021**, *60*, 5607, https://doi.org/10.1021/acs.inorgchem.0c03554
7	GETFOD	$\{Co^{II}_{16}\}$	Metallocages	Antiferromagnetic $Co^{II}\cdots Co^{II}$ exchange interactions	X. Zhu, Sh. Wang, H. Han, X. Hang, W. Xie, W. Liao, *Cryst. Growth Des*., **2018**, *18*, 225, https://doi.org/10.1021/acs.cgd.7b01127
8	HASSIH	$\{Co^{II}_{16}\}$	Metallocages		G. Zhang, H. Han, K. Li, H. Zhang, W. Liao, *Zeitschrift fur Naturforschung,B:Chemical Sciences*, **2021**, *76*, 827, https://doi.org/10.1515/znb-2021-0138
9	HASSON				
10	HIPHOF	$\{Co^{II}_{16}\}$	Metallocages	Cavity-specific binding properties in both solid state and solution	F.-R. Dai, D. C. Becht, Zh. Wang, *Chem. Commun*., **2014**, *50*, 5385, https://doi.org/10.1039/C3CC47420H
11	HITGOH	$\{Co^{II}_{16}\}$	"Clusters of clusters"		M. Rodriguez-Zubiri, V. Gallo, J. Rose, R. Welter, P. Braunstein, *Chem. Commun*., **2008**, 64, https://doi.org/10.1039/B713540H
12	JIGSOK	$\{Co^{II}_{16}\}$	Metallocages	Proton receptor	Ch.-Zh. Sun, L.-J. Cheng, Y. Qiao, L.-Y. Zhang, Zh.-N. Chen, F.-R. Dai, W. Lin, Zh. Wang, *Dalton Trans*., **2018**, *47*, 10256, https://doi.org/10.1039/C8DT01900B
13	KULNIP	$\{Co^{II}_{16}\}$	Metallocages		J. Liu, A. Wei, *Chem. Commun*., **2009**, 4254, https://doi.org/10.1039/B903954F
14	LINQOS	$\{Co^{II}_{16}\}$	Metallocages		M. R. Dworzak, Ch. M. Montone, N. I. Halaszynski, G. P. A. Yap,

15	LINQUY				Ch. J. Kloxin, E. D. Bloch, *Chem. Commun.*, **2023**, *59*, 8977. https://doi.org/10.1039/D3CC02015K
16	MUBSUX	$\{Co^{II}_{16}\}$	Metallocages		D. Eisler, W. Hong, M. C. Jennings, R. J. Puddephatt, *Organometallics*, **2002**, *21*, 3955, https://doi.org/10.1021/om020394y
17	NESYAP	$\{Co^{II}_{16}\}$	Wheel-like cluster	Weak ferromagnetic nearest neighbour exchange interactions	P. A. Tsami, T. G. Tziotzi, A. B. Canaj, M. K. Singh, S. J. Dalgarno, E. K. Brechin, C. J. Milios, *Dalton Trans.*, **2022**, 51, 15128, https://doi.org/10.1039/D2DT02554J
18	PEFXEF	$\{Co^{II}_{16}\}$	Metallocages	Strong antiferromagnetic $Co^{II}\cdots Co^{II}$ exchange interactions	K. Xiong, F. Jiang, Y. Gai, Zh. He, D. Yuan, L. Chen, K. Su, M. Hong, *Cryst. Growth Des.*, **2012**, *12*, 3335, https://doi.org/10.1021/cg300483c
19	PEZCIK	$\{Co^{II}_{16}\}$	Metallocages		X. Hang, X. Wang, M. Wang, M. Chen, Y. Bi, *Inorg. Chem. Frontiers*, **2022**, *10*, 926, https://doi.org/10.1039/D2QI01885C
20	RAFDAH	$\{Co^{II}_{16}\}$	Metallocages based on calixarene derivatives	Proton-conducting material	G. Zhang, M. Wei, H. Zang, H. Zhang, W. Liao, *Inorg. Chim. Acta*, **2021**, *514*, 120027, https://doi.org/10.1016/j.ica.2020.120027
21	RAFDEL				
22	SAQSEK	$\{Co^{II}_{16}\}$	Square-shape metallomacrocycle based on polytriazolate ligands	Dominant antiferromagnetic inter-actions within the cluster.	W.-Q. Lin, J.-D. Leng, M.-L. Tong, *Chem. Commun.*, **2012**, *48*, 4477, https://doi.org/10.1039/C2CC31141K
23	TAKCIU	$\{Co^{II}_{16}\}$	Metallocages based on calixarene derivatives	Adsorption properties	X. Hang, Sh. Wang, X. Zhu, H. Han, W. Liao, *CrystEngComm*, **2016**, *18*, 4938, https://doi.org/10.1039/C6CE00028B
24	TAKCOA				
25	TAKCUG				
26	TAKDAN				
27	TIYNAS	$\{Co^{II}_{16}\}$	Wheel-shaped cluster	Ferromagnetic cubes antiferromagnetically coupled to the squares within the cluster	Y.-Q. Hu, M.-H. Zeng, K. Zhang, Sh. Hu, F.-F. Zhou, M. Kurmoo, *J. Am. Chem. Soc.*, **2013**, *135*, 7901, https://doi.org/10.1021/ja3123784
28	WEBZIO	$\{Co^{II}_{16}\}$	Metallocages based on calixarene derivatives	Adsorption properties	M. Liu, W. Liao, *CrystEngComm*, **2012**, *14*, 5727, https://doi.org/10.1039/C2CE25692D
29	WEBZOU				
30	WIZZIQ	$\{Co^{II}_{16}\}$	Metallocages based on calixarene derivatives	Antiferromagnetic $Co^{II}\cdots Co^{II}$ exchange interactions	M. Liu, Sh. Du, Y. Bi, W. Liao, *Inorg. Chem. Commun.*, **2014**, *41*, 96, https://doi.org/10.1016/j.inoche.2014.01.009
31	YEHVOZ	$\{Co^{II}_{16}\}$	Metallocages based on calixarene derivatives	Adsorption properties	G. Zhang, X. Zhu, M. Liu, W. Liao, *J. Mol. Struct.*, **2018**, *1151*, 29, https://doi.org/10.1016/j.molstruc.2017.09.024

Table S2. Crystal data and structure refinement details for compounds **1-2**

	1	**2**
Empirical formula	$C_{102}H_{205}Co_{16}NO_{66}$	$C_{106}H_{213}Co_{16}NO_{66}$
Formula weight / g mol^{-1}	3444.54	3500.64
Temperature / K	293(2)	293(2)
Wavelength / Å	0.71073	0.71073
Crystal system	monoclinic	monoclinic
Space group	$P2_1/c$	$P2_1/c$
Unit cell dimensions		
a / Å	19.4844(5)	19.5755(6)
b / Å	19.7970(6)	19.8822(9)
c / Å	20.2908(10)	20.6464(11)
α / °	90	90
β / °	93.527(3)	94.644(3)
γ / °	90	90
Volume / Å^3	7812.0(5)	8009.3(6)
Z	2	2
Density (calculated) / Mg m^{-3}	1.464	1.452
Absorption coefficient / mm^{-1}	1.731	1.690
F(000)	3568	3632
Crystal size / mm^3	0.30 × 0.20 × 0.10	0.35 × 0.35 × 0.20
Theta range for data collection	2.996 to 25.049	2.943 to 25.249
Index ranges	$-20 \le h \le 23$, $-21 \le k \le 23$, $-14 \le l \le 24$	$-22 \le h \le 23$, $-23 \le k \le 14$, $-16 \le l \le 24$
Reflections collected	27514	26859
Independent reflections	13746 [R_{int} = 0.0525]	14469 [R_{int} = 0.0464]
Completeness to theta = 25.049°	99.2%	99.7%
Data / restraints / parameters	13746 / 801 / 1030	14469 / 212 / 974
Goodness-of-fit on F^2	1.000	1.003
Final R indices [$I > 2\sigma(I)$]	R_1 = 0.0630, wR_2 = 0.1209	R_1 = 0.0733, wR_2 = 0.1782
R indices (all data)	R_1 = 0.1348, wR_2 = 0.1436	R_1 = 0.1414, wR_2 = 0.2143
Largest diff. peak and hole / e·Å^{-3}	0.755 and –0.473	1.013 and –0.810

Table S3. Selected bond distances (in Å) for **1-2**

1			
Co1–O29	1.899(3)	Co5–O11	2.017(4)
Co1–O30	1.902(4)	Co5–O25	2.069(5)
Co1–O26	1.902(4)	Co5–O14	2.099(3)
Co1–O28	1.903(3)	Co5–O28	2.126(4)
Co1–O1	1.906(3)	Co5–O12	2.135(4)
Co1–O31	1.910(3)	Co5–O30	2.146(3)
Co2–O4	2.021(5)	Co6–O2	2.000(3)
Co2–O24	2.034(4)	Co6–O16	2.048(4)
Co2–O26	2.117(3)	Co6–O1	2.099(3)
Co2–O22	2.135(4)	Co6–O14	2.127(4)
Co2–O31	2.146(4)	Co6–O30	2.153(3)
Co2–O6	2.150(4)	Co6–O18	2.181(3)
Co3–O8	1.987(4)	Co7–O20	2.074(4)
Co3–O5	2.002(5)	Co7–O18	2.096(4)
Co3–O26	2.113(3)	Co7–O1	2.099(3)
Co3–O6	2.118(4)	Co7–O31	2.106(3)
Co3–O29	2.151(4)	Co7–O3	2.116(3)
Co3–O27	2.224(4)	Co7–O22	2.117(4)
Co4–O9	1.998(4)	Co8–O2$^{\#1}$	2.049(3)
Co4–O10	2.009(4)	Co8–O2	2.050(3)
Co4–O12	2.118(4)	Co8–O15	2.060(4)
Co4–O28	2.122(3)	Co8–O17	2.110(4)
Co4–O29	2.146(3)	Co8–O19	2.112(4)
Co4–O27	2.204(4)	Co8–O3	2.118(3)
2			
Co1–O26	1.899(4)	Co5–O11	2.015(5)
Co1–O28	1.903(4)	Co5–O25	2.054(5)
Co1–O30	1.907(4)	Co5–O14	2.102(4)
Co1–O31	1.907(4)	Co5–O28	2.119(4)
Co1–O29	1.913(4)	Co5–O12	2.127(4)
Co1–O1	1.920(4)	Co5–O29	2.152(4)
Co2–O24	2.033(5)	Co6–O2	2.008(4)
Co2–O4	2.037(5)	Co6–O16	2.056(5)
Co2–O26	2.116(4)	Co6–O1	2.099(4)
Co2–O22	2.127(4)	Co6–O14	2.121(4)
Co2–O31	2.145(4)	Co6–O29	2.156(4)
Co2–O6	2.153(5)	Co6–O18	2.176(4)
Co3–O5	1.996(6)	Co7–O20	2.074(4)
Co3–O8	2.011(5)	Co7–O18	2.081(4)
Co3–O6	2.114(5)	Co7–O1	2.095(4)
Co3–O26	2.117(4)	Co7–O22	2.105(5)
Co3–O30	2.141(4)	Co7–O31	2.107(4)
Co3–O27	2.226(5)	Co7–O3	2.115(4)
Co4–O9	1.994(5)	Co8–O2$^{\#1}$	2.044(4)

Co4–O10	2.015(5)	Co8–O2	2.055(3)
Co4–O28	2.104(4)	Co8–O15$^{\#1}$	2.067(5)
Co4–O12	2.120(5)	Co8–O17	2.108(5)
Co4–O30	2.144(4)	Co8–O19	2.109(5)
Co4–O27	2.201(5)	Co8–O3	2.118(4)
Symmetry transformations used to generate equivalent atoms: #1 -x+1,-y+1,-z+1			

Table S4. Hydrogen bonds geometry (Å, deg) for **1-2**

D–H···A	d(D–H)	d(H···A)	d(D···A)	<(DHA)
1				
O1–H1...O32	0.83	2.04	2.796(6)	151.5
O2–H2A...O32	0.83	2.27	3.029(7)	151.4
O3–H3D...O23	0.85	1.83	2.577(6)	145.3
O3–H3E...O21	0.85	1.78	2.558(6)	151.5
O24–H24D...O7	0.842(19)	1.88(3)	2.665(6)	154(4)
O24–H24E...O20	0.843(19)	1.99(3)	2.754(5)	151(5)
O25–H25D...O16	0.854(19)	2.04(2)	2.844(5)	155(3)
O25–H25E...O13	0.862(19)	1.86(2)	2.677(6)	157(3)
O27–H27...O33	0.83	1.80	2.596(6)	161(5)
O32–H32H...O17	0.887(15)	2.135(15)	2.992(6)	162(2)
O32–H32J...N1	0.855(19)	2.07(2)	2.819(16)	146(5)
O33–H33A...O13$^{\#2}$	0.86(2)	1.99(3)	2.834(7)	165(8)
O33–H33B...O7$^{\#3}$	0.854(19)	2.124(19)	2.862(6)	145(4)
2				
O1–H1...O32	0.83	2.03	2.788(7)	151.1
O2–H2A...O32	0.83	2.28	3.036(8)	150.8
O3–H3D...O21	0.85	1.79	2.569(7)	151.3
O3–H3E...O23	0.85	1.83	2.568(7)	144.2
O24–H24D...O7	0.853(19)	1.87(3)	2.671(7)	154(4)
O24–H24E...O20	0.841(19)	1.97(3)	2.752(6)	151(5)
O25–H25D...O16	0.841(18)	2.13(4)	2.823(6)	155(3)
O25–H25E...O13	0.841(19)	1.95(4)	2.664(7)	157(3)
O27–H27...O33	0.83	1.83	2.618(6)	161(5)
O32–H32H...N1	0.864(18)	2.110(19)	2.940(15)	162(2)
O32–H32J...O17	0.887(16)	2.141(15)	2.999(7)	146(5)
O33–H33A...O13$^{\#2}$	0.866(18)	2.118(19)	2.934(8)	165(8)
O33–H33B...O7$^{\#3}$	0.857(18)	2.109(18)	2.934(8)	145(4)
Symmetry transformations used to generate equivalent atoms: #1 -x+1,-y+1,-z+1 #2 x,-y+3/2,z+1/2 #3 -x+2,y+1/2,-z+3/2				

Table S5. BVS calculations for Co atoms in **1–2**

Atom	BVS value*			Oxidation state
	a	*b*	*c*	
1				
Co1	2.91	3.46	3.11	**+3**
Co2	2.02	1.99	1.86	**+2**
Co3	2.03	2.00	1.87	**+2**
Co4	2.04	2.01	1.88	**+2**
Co5	2.04	2.01	1.88	**+2**
Co6	2.01	1.98	1.85	**+2**
Co7	1.98	1.95	1.82	**+2**
Co8	2.08	2.05	1.91	**+2**
2				
Co1	2.88	3.41	3.08	**+3**
Co2	2.00	1.97	1.84	**+2**
Co3	2.03	2.00	1.87	**+2**
Co4	2.05	2.02	1.88	**+2**
Co5	2.04	2.01	1.87	**+2**
Co6	2.00	1.97	1.84	**+2**
Co7	2.01	1.98	1.85	**+2**
Co8	2.09	1.92	1.92	**+2**

∗Values of R_0 for Co–O bonds for oxidation states +3 R_0 = 1.637(*a* [1]) and 1.70 (*b* [2]) and +2 R_0 = 1.691(*a* [1]) and 1.685 (*b* [2]). R_0 = 1.661 for oxidation states of Co(II) and Co(III) (*c* [1])

[1] Wood, R. M.; Palenik, G. J. Bond Valence Sums in Coordination Chemistry. A Simple Method for Calculating the Oxidation State of Cobalt in Complexes Containing Only Co-O Bonds. *Inorg. Chem.* **1998**, *37*, 4149-4151.

[2] Brese, N. E.; O'Keeffe, M. Bond-valence parameters for solids. *Acta Crystallogr., Sect. B* **1991**, *B47*, 192-197.

Table S6. Hirshfeld surfaces for the Co(II) and Co(III) centers in **1**

HS	**Co(III)**	**Co(II)**						
	Co1	Co2	Co3	Co4	Co5	Co6	Co7	Co8
d_i	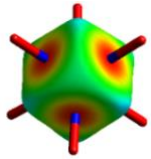	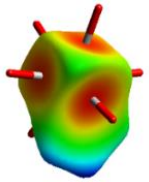	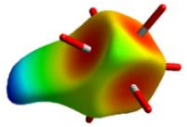	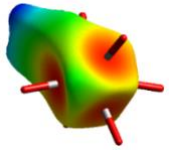	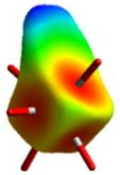	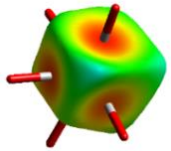	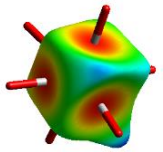	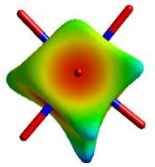
d_e	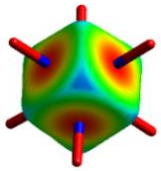	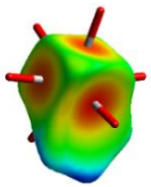	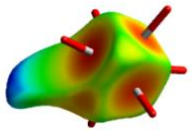	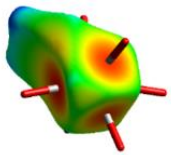	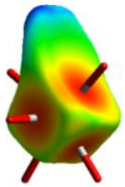	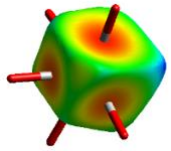	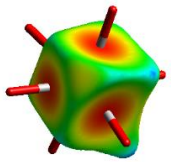	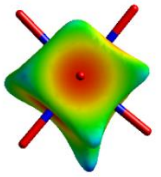
d_{norm}	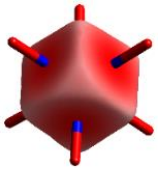	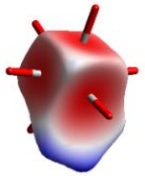	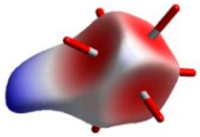	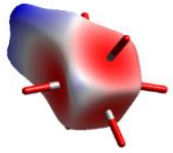	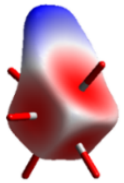	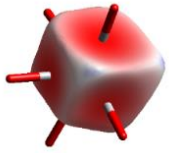	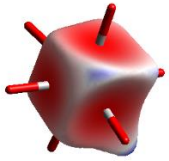	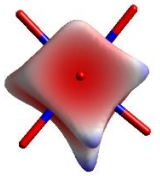
Shape	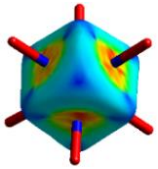	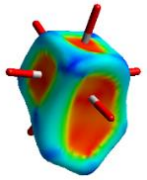	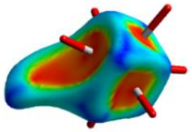	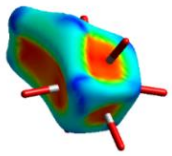	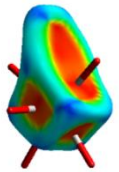	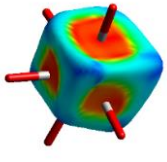	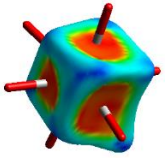	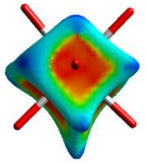
Curvedness	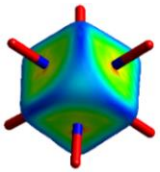	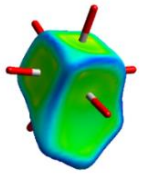	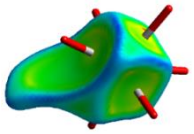	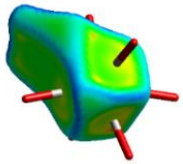	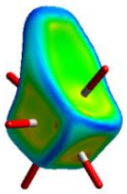	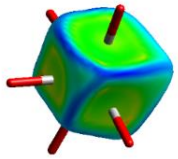	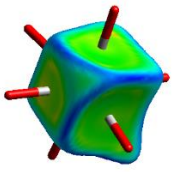	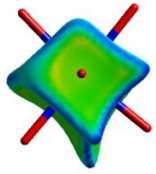

Table S7. Hirshfeld surfaces for the Co(II) and Co(III) centers in **2**

HS	**Co(III)**	**Co(II)**						
	Co1	Co2	Co3	Co4	Co5	Co6	Co7	Co8
d_i	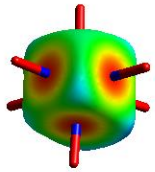	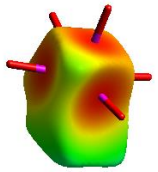	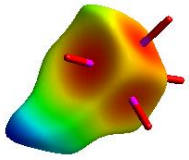	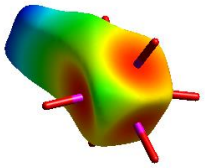	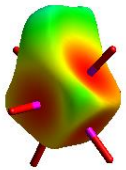	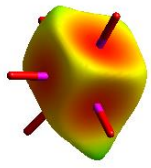	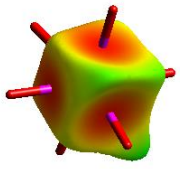	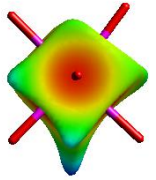
d_e	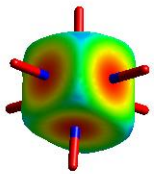	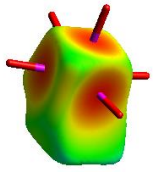	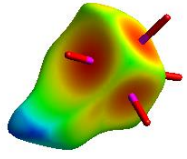	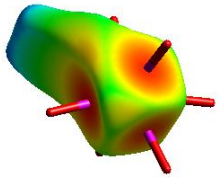	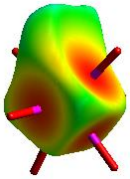	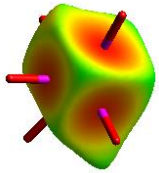	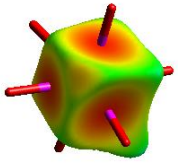	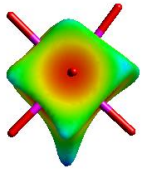
d_{norm}	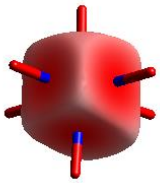	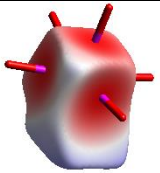	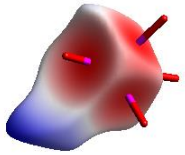	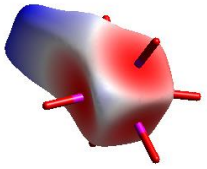	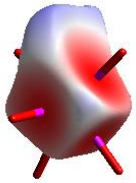	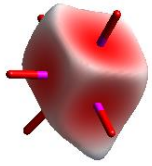	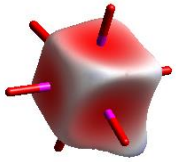	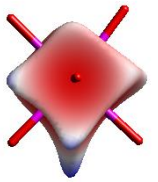
Shape	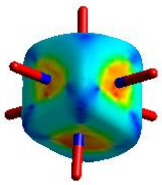	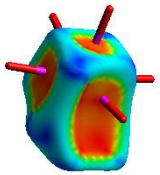	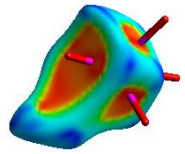	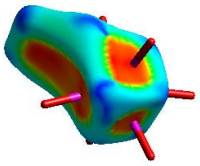	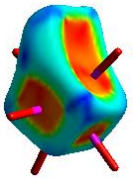	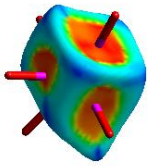	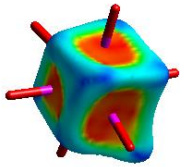	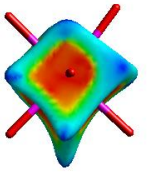
Curvedness	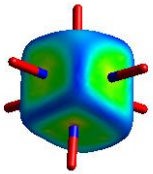	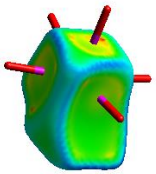	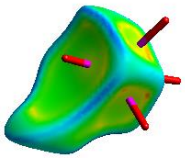	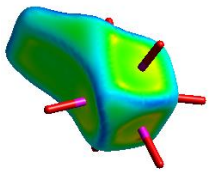	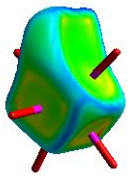	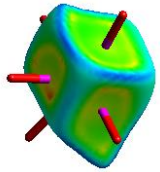	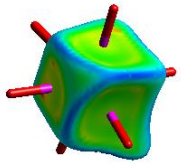	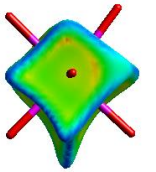

Table S8. Quantitative data from Hirshfeld surface of the Co(II) and Co(III) centers in **1-2**

Co centers	Volume / $Å^3$	Area / $Å^2$	Globularity	Asphericity
1				
Co1 (Co^{III})	7.13	20.05	0.894	0.006
Co2 (Co^{II})	12.44	32.83	0.791	0.038
Co3 (Co^{II})	13.20	35.10	0.770	0.103
Co4 (Co^{II})	12.80	34.32	0.771	0.055
Co5 (Co^{II})	12.83	35.16	0.754	0.089
Co6 (Co^{II})	11.23	28.76	0.843	0.019
Co7 (Co^{II})	11.63	29.82	0.833	0.022
Co8 (Co^{II})	11.66	31.37	0.793	0.005
2				
Co1 (Co^{III})	7.16	20.08	0.895	0.006
Co2 (Co^{II})	12.62	33.10	0.792	0.036
Co3 (Co^{II})	13.40	35.96	0.759	0.128
Co4 (Co^{II})	13.60	37.18	0.741	0.097
Co5 (Co^{II})	12.34	32.88	0.786	0.036
Co6 (Co^{II})	11.10	28.26	0.851	0.011
Co7 (Co^{II})	11.64	29.94	0.830	0.016
Co8 (Co^{II})	11.65	31.27	0.795	0.005

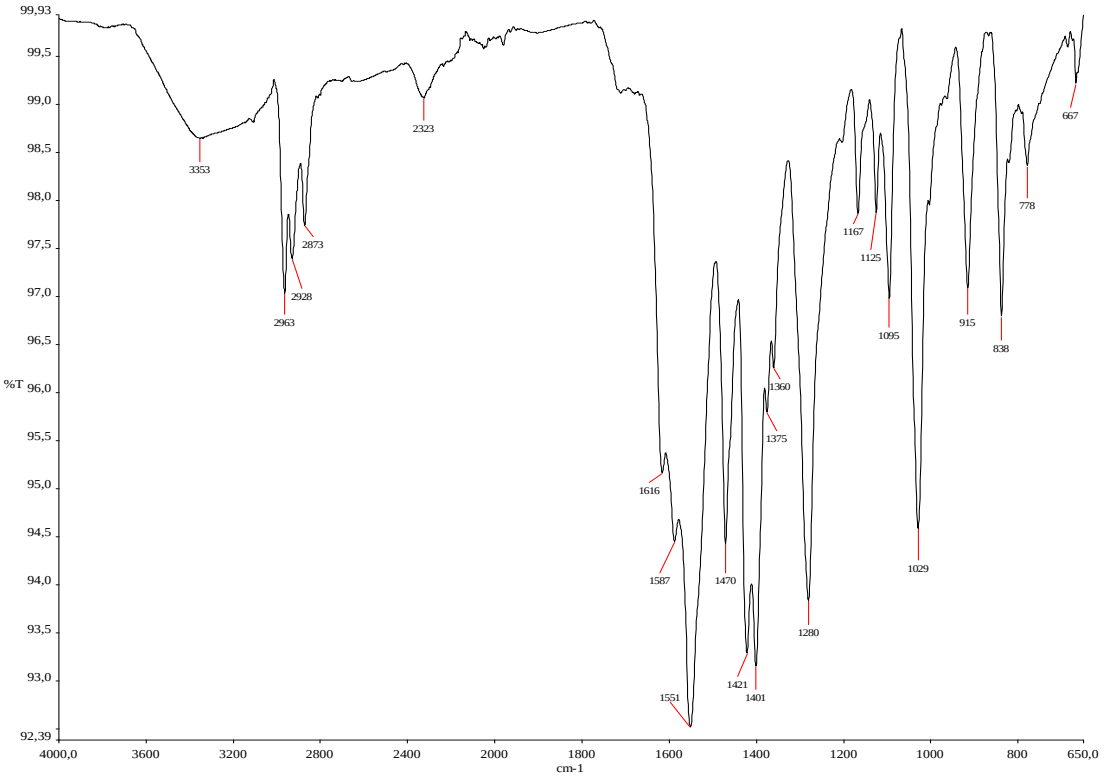

Figure S1. IR spectrum of **1**.

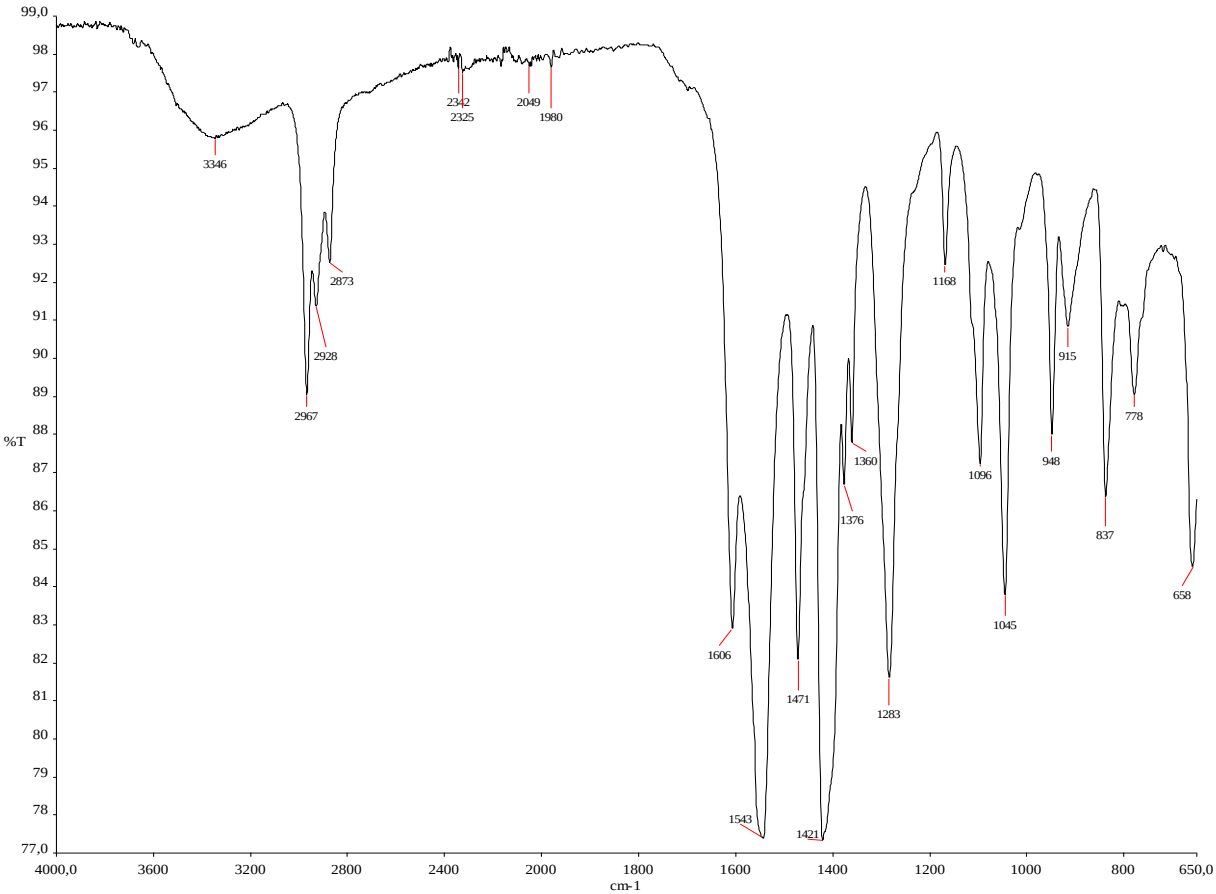

Figure S2. IR spectrum of **2**.

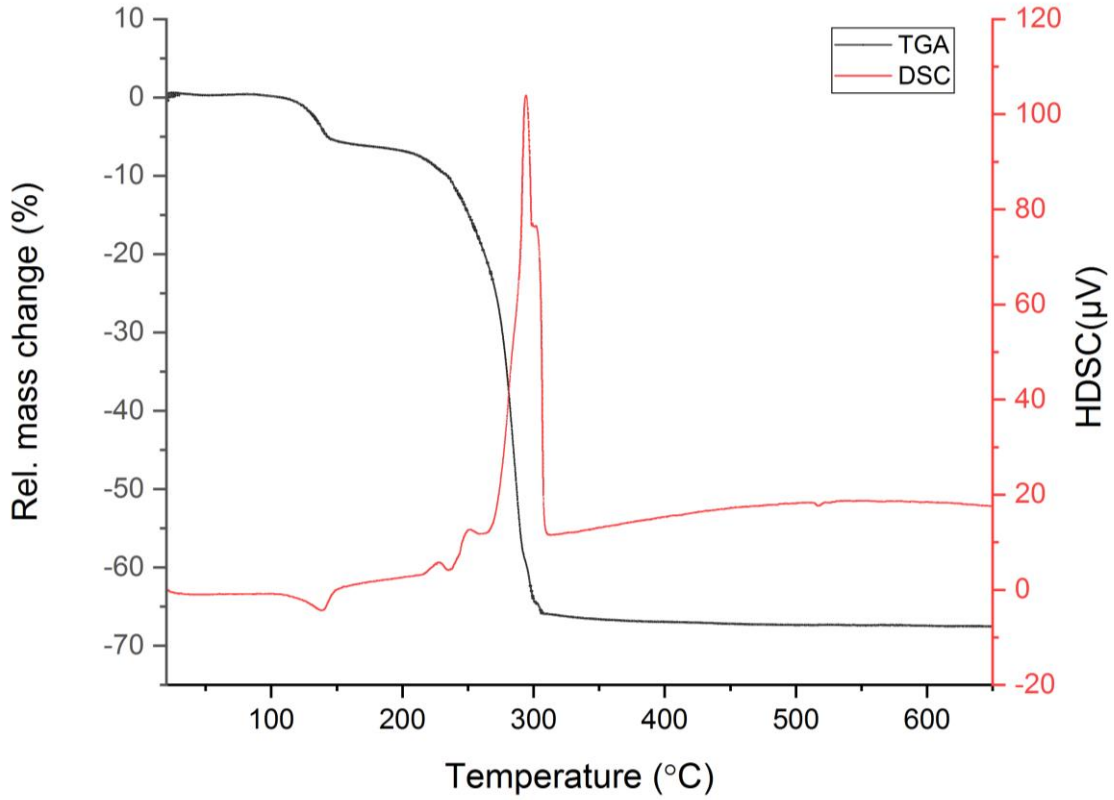

Figure S3. TGA/DSC curves for **1**.

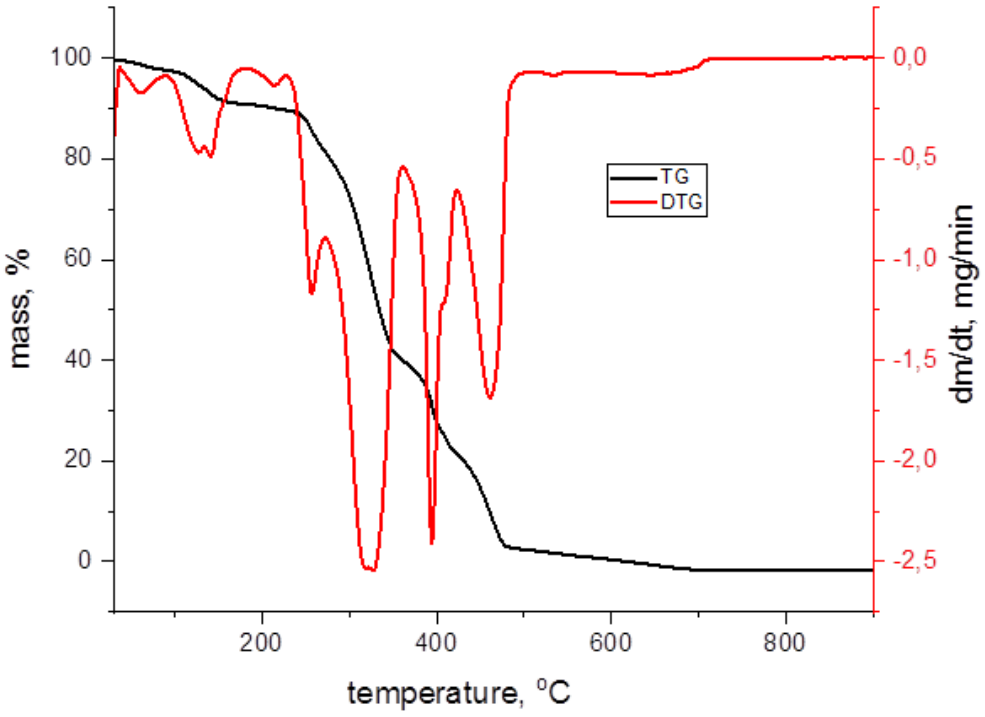

Figure S4. TG/DTG curves for **2**.

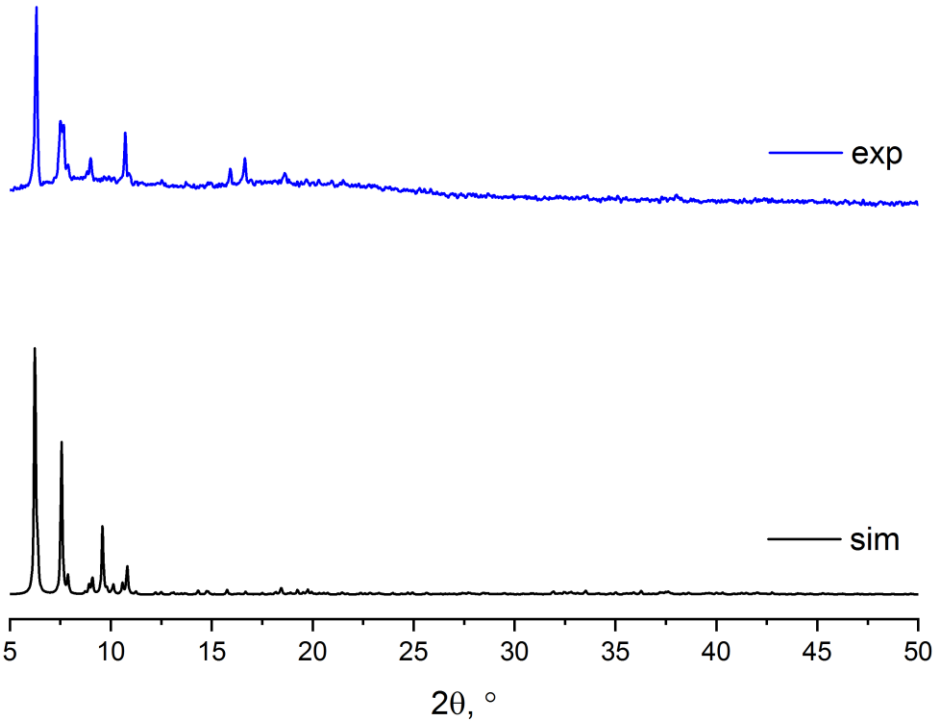

Figure S5. PXRD analysis of **1**.

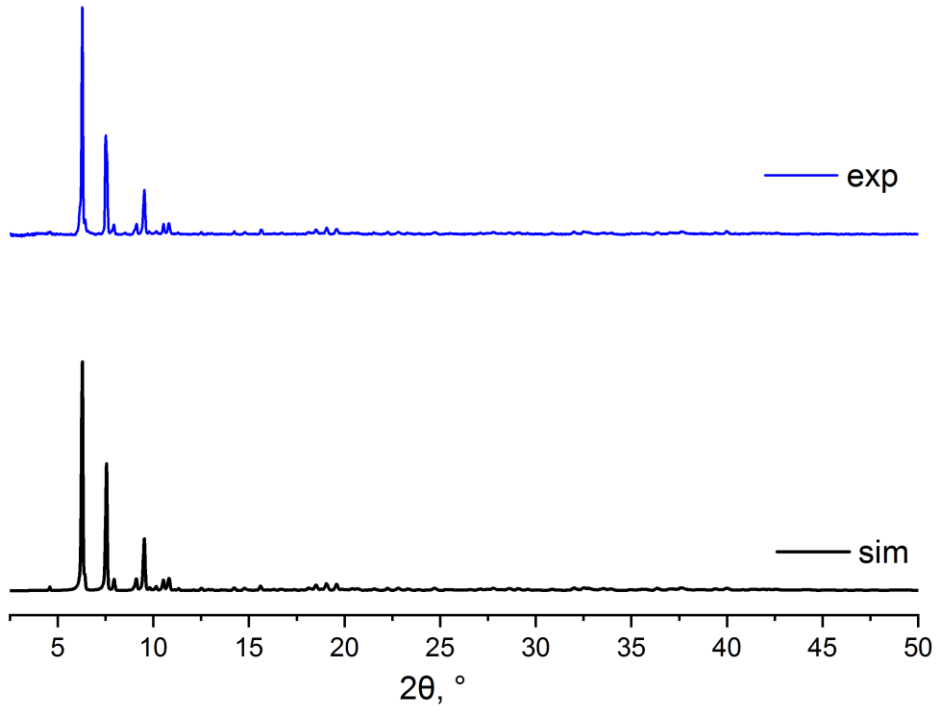

Figure S6. PXRD analysis of **2**.

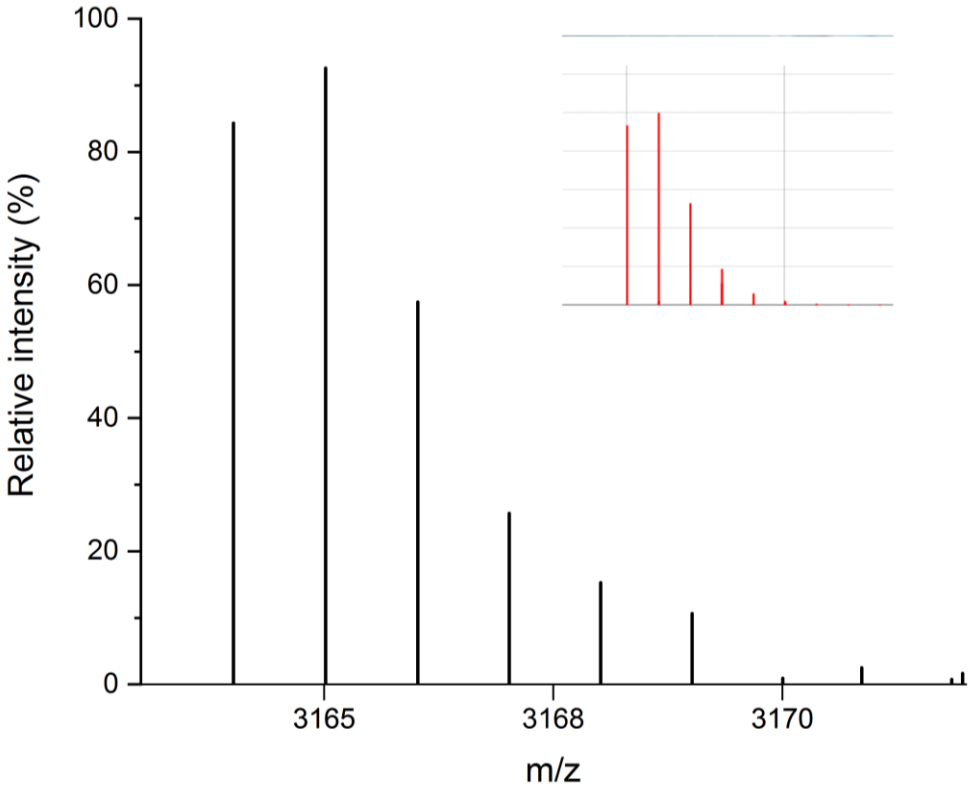

Figure S7. Experimental and simulated (insert) isotope patterns for the anionic fragment: $[Co^{II}_{14}Co^{III}_{2}O_2(OH)_2(ib)_{19}(thme)_2(Hthme)_2(MeOH)]^-$ (*m*/*z* 3165.01, 100%) in **1**.

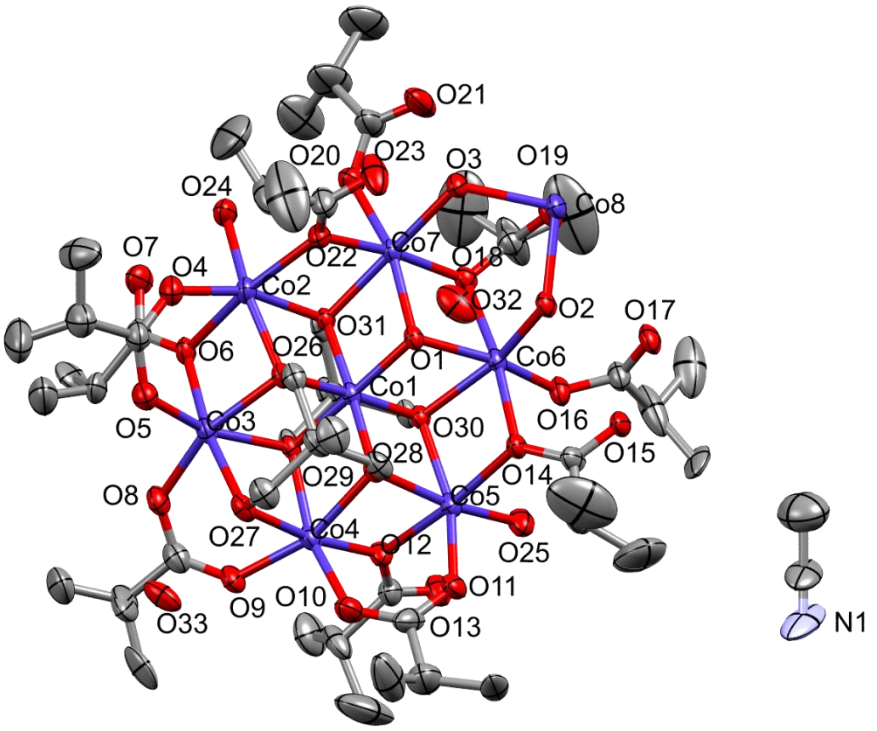

Figure 8. Asymmetric unit of nanocluster **1**, with a partial atom labeling and displacement ellipsoids drawn at the 30% probability level. Hydrogen atoms are omitted for clarity.

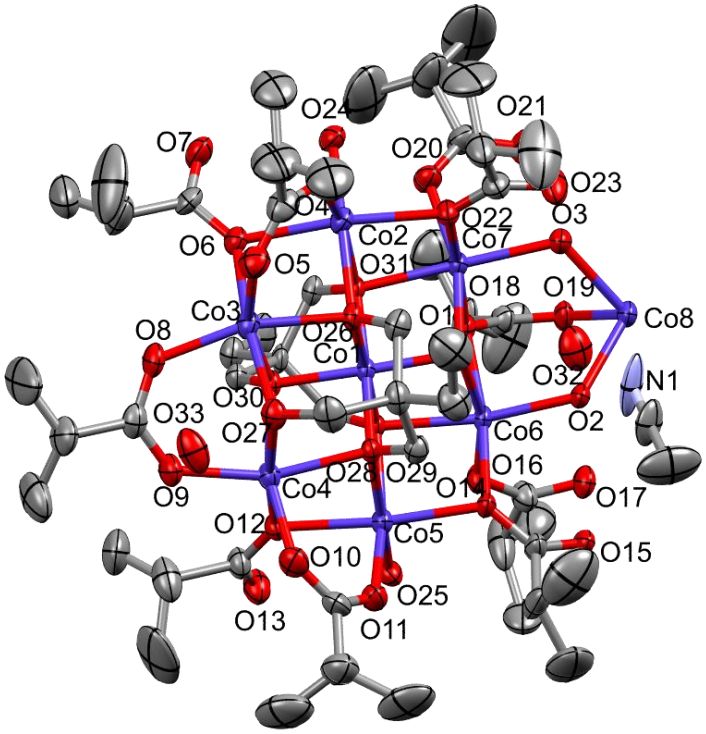

Figure S9. Asymmetric unit of nanocluster **2**, with a partial atom labeling and displacement ellipsoids drawn at the 30% probability level. Hydrogen atoms are omitted for clarity.

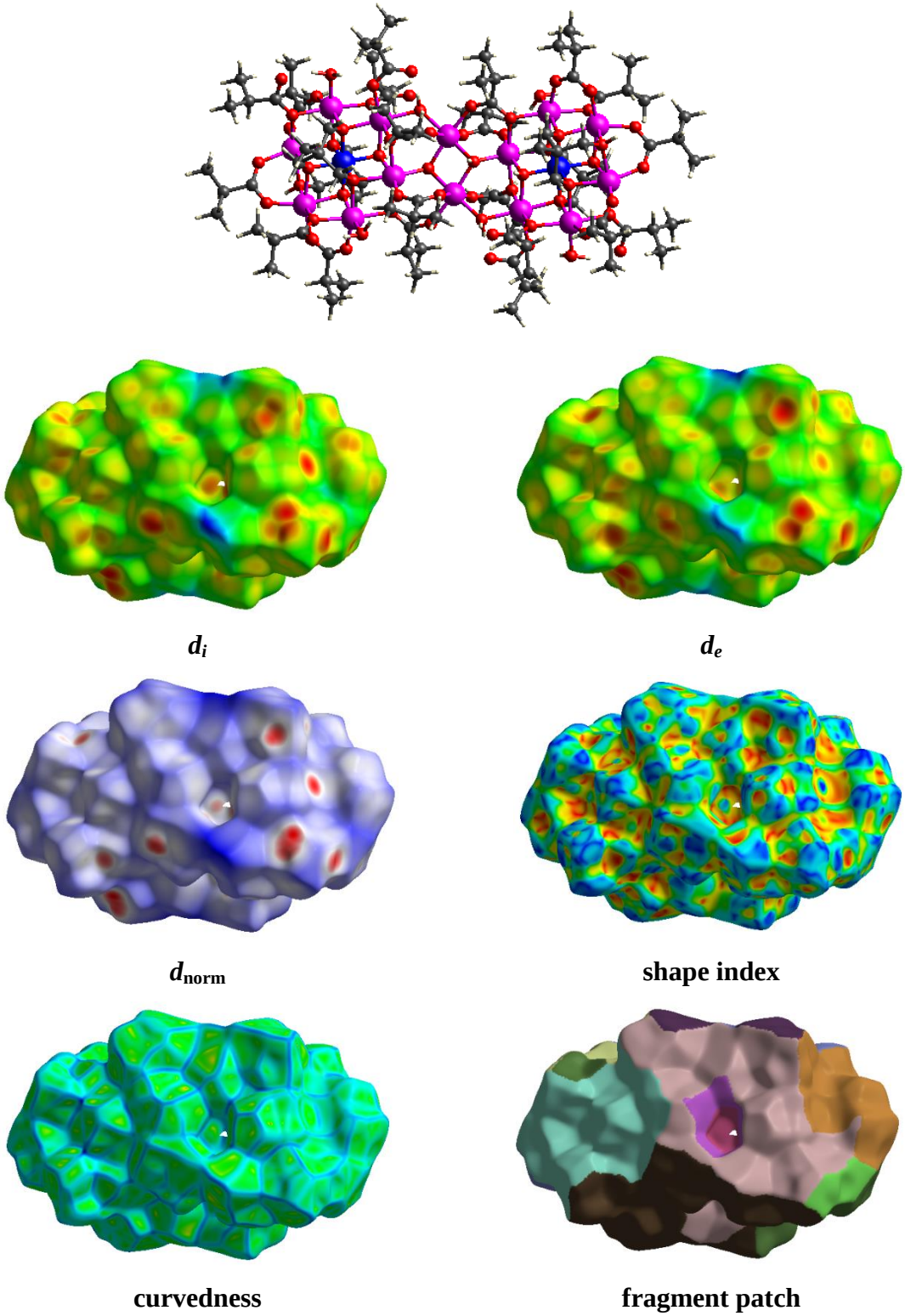

Figure S10. View of the Hirshfeld surface for $[Co_{16}(OH)_4(ib)_{20}(thme)_2(Hthme)_2(H_2O)_6]$ cluster in **1** colour-coded with different properties.

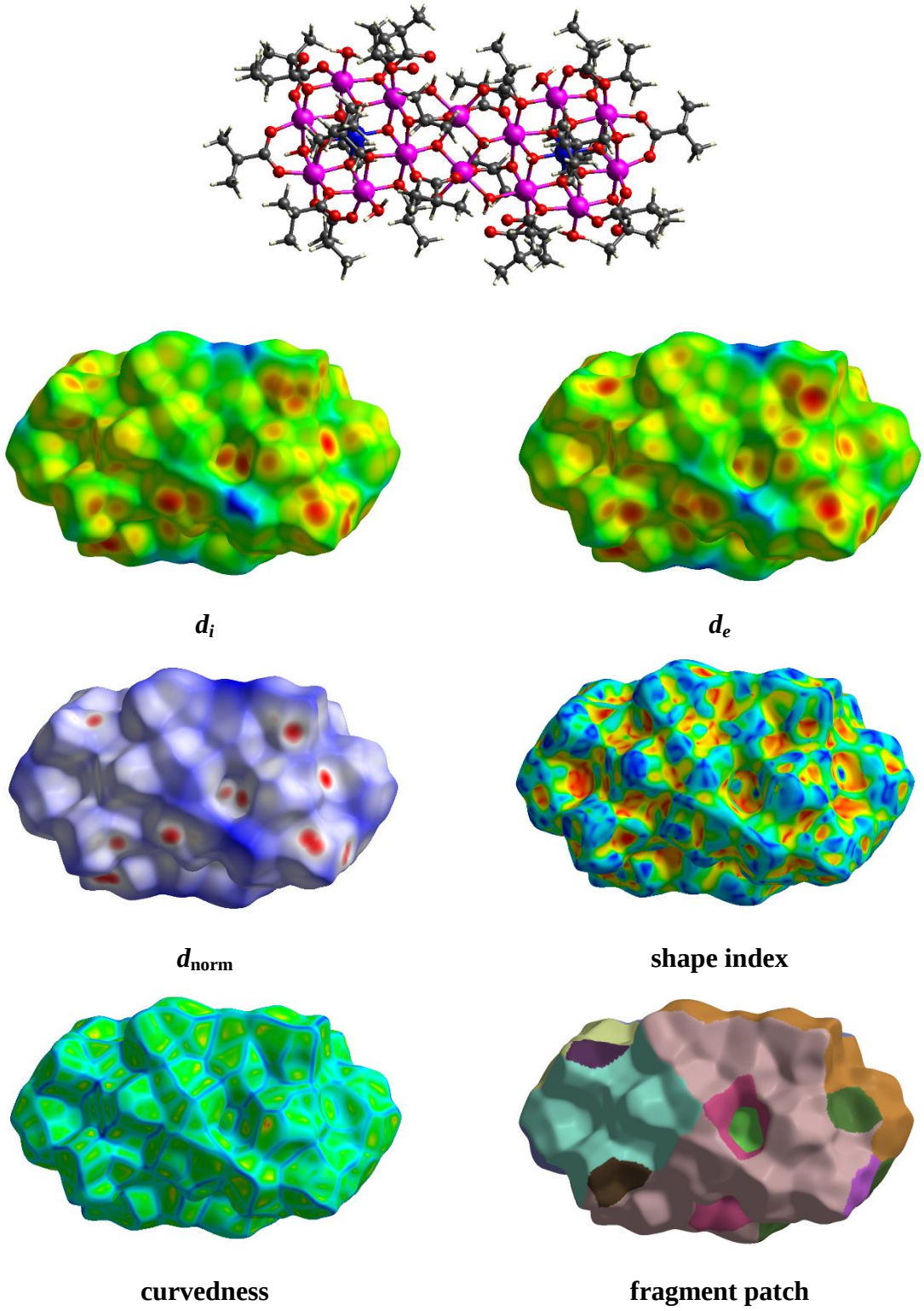

Figure S11. View of the Hirshfeld surface for $[Co_{16}(OH)_4(ib)_{20}(thmp)_2(Hthmp)_2(H_2O)_6]$ cluster in **2** colour-coded with different properties.

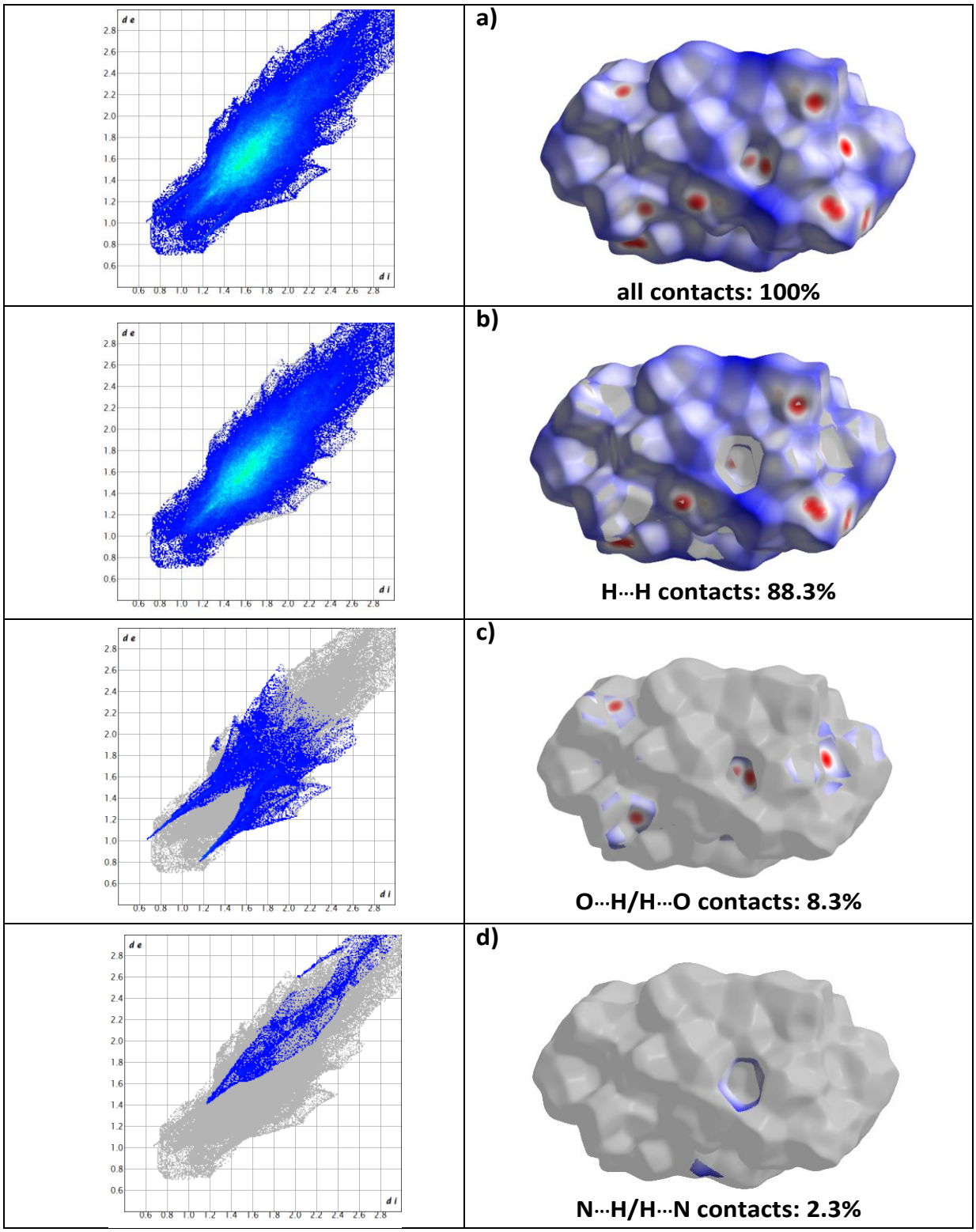

Figure S12. 2D fingerprint plots (d_e *vs.* d_i) and d_{norm} surface plots of the {Co_{16}} cluster in **2**. Short contacts are represented by red areas, long contacts by blue areas, and the white area represents contacts with lengths equivalent to the sum of the van der Waal radii of the interacting atoms. a) d_{norm} distribution of all interactions, b) H···H, c) O···H/H···O, and d) N···H/H···N contacts. Surfaces to the right highlight the relevant d_{norm} surface patches associated with the specific contacts. The percentage of contribution is specified for each contact.

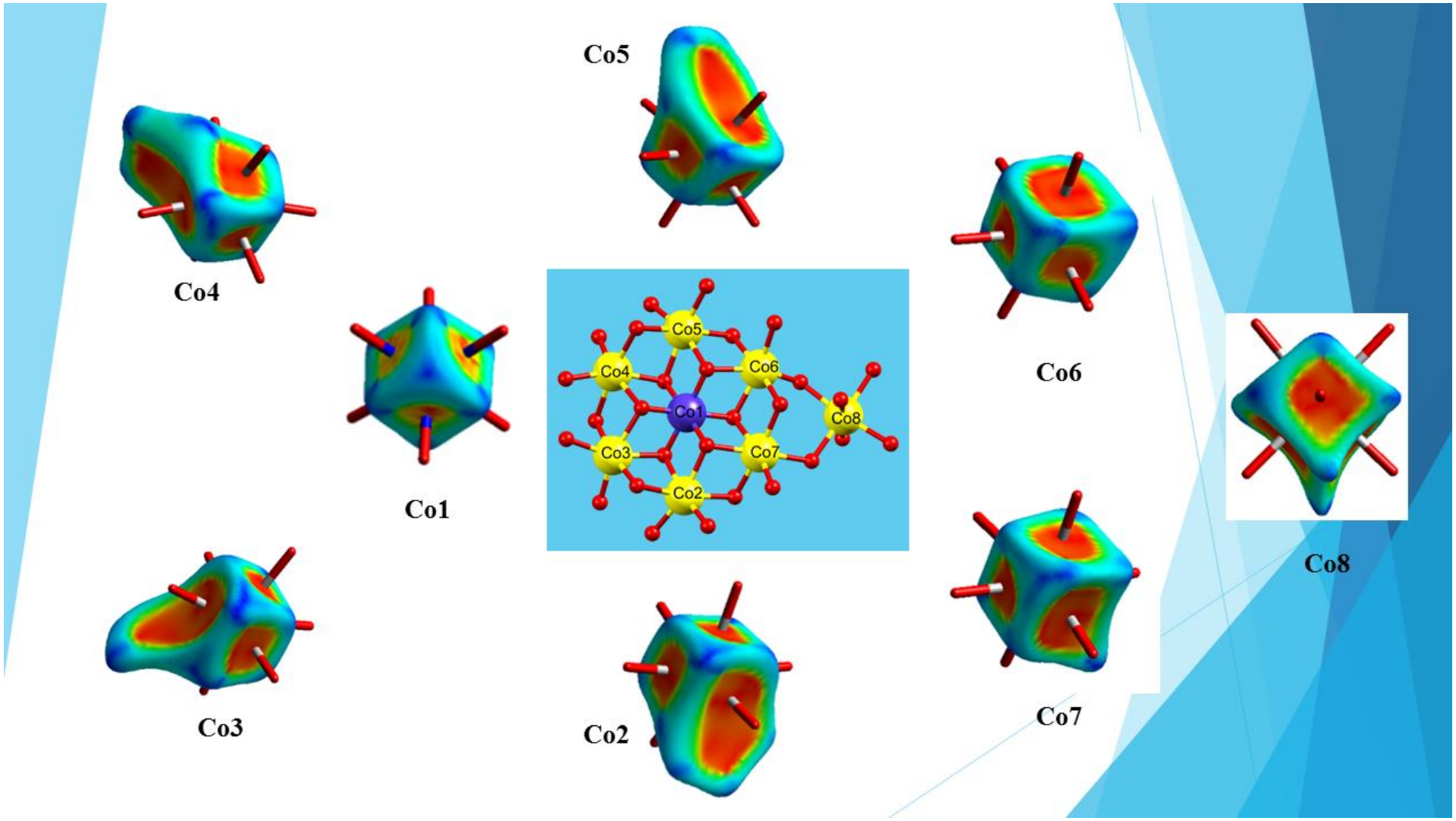

Figure S13. Hirshfeld surfaces for the Co(III) and Co(II) centres presenting different shapes in **1**.

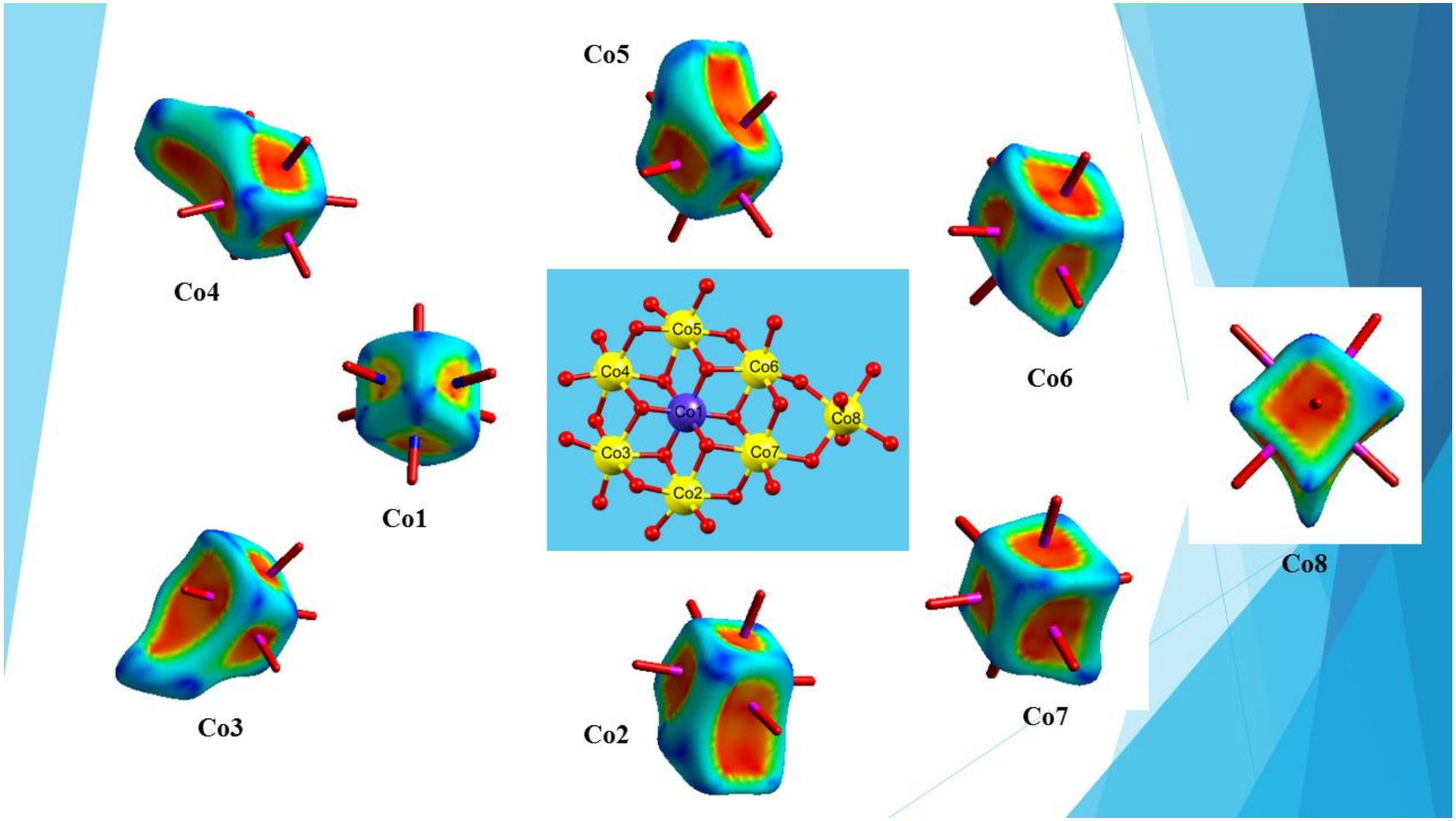

Figure S14. Hirshfeld surfaces for the Co(III) and Co(II) centres presenting different shapes in **2**.